

# Green synthesis of silver nanoparticles using green tea leaves: Experimental study on the morphological, rheological and antibacterial behaviour

Maryam Nakhjavani<sup>1</sup> · V. Nikkhah<sup>2</sup> · M. M. Sarafraz<sup>2</sup> · Saeed Shoja<sup>3</sup> · Marzieh Sarafraz<sup>4</sup>

Received: 24 October 2016 / Accepted: 15 May 2017 / Published online: 29 May 2017  
© Springer-Verlag Berlin Heidelberg 2017

**Abstract** In this paper, silver nanoparticles are produced via green synthesis method using green tea leaves. The introduced method is cost-effective and available, which provides condition to manipulate and control the average nanoparticle size. The produced particles were characterized using x-ray diffraction, scanning electron microscopic images, UV visualization, digital light scattering, zeta potential measurement and thermal conductivity measurement. Results demonstrated that the produced samples of silver nanoparticles are pure in structure (based on the x-ray diffraction test), almost identical in terms of morphology (spherical and to some extent cubic) and show longer stability when dispersed in deionized water. The UV-visualization showed a peak in 450 nm, which is in accordance with the previous studies reported in the literature. Results also showed that small particles have higher thermal and antimicrobial performance. As green tea leaves are used for extracting the silver nanoparticles, the method is eco-friendly. The thermal behaviour of silver nanoparticle was also analysed by dispersing the nanoparticles inside the deionized water. Results showed that thermal conductivity of the silver

nano-fluid is higher than that of obtained for the deionized water. Activity of Ag nanoparticles against some bacteria was also examined to find the suitable antibacterial application for the produced particles.

**Keywords** Silver nanoparticles · Eco-friendly nanofluid · Antimicrobial behaviour · Thermal conductivity measurement

## 1 Introduction

Plant extraction technique is one of the practical methods that has widely been used for producing the metallic nanoparticles including silver, iron platinum and gold [1–4]. This method not only is the cost-effective and available technique for producing nanoparticles but also it offers special flexibility regarding the morphology, size and quality of the extracted particles [5]. The produced particles can be implemented for different industrial, medical and scientific applications. When it comes to extraction of metallic particles using plants, some antimicrobial, antiseptic, antihelmintic and antinociceptive activities for the particles should be taken into account. For instance, some herbs and natural compounds such as cannonball trees were traditionally used for skin diseases and malaria [6], while Alginates were extensively used for wound healing and antibacterial applications.

Nanotechnology emerges a bright future towards the medical application of biologically produced nanoparticles such as silver obtained by plant extraction methods via hygienic plants. Green synthesis of metallic particles such as silver nanoparticles is one of the promising options for obtaining the size-controlled nanoparticles with antibacterial activity [7–9].

Recently, in a study conducted by Wang et al. [10], AgNPs were synthesized using the cell filtrate of *C. militaris* mycelium as reducing agents. The formation of AgNPs was first confirmed by the surface plasmon resonance illustrated in

✉ M. M. Sarafraz  
mohamadmohsensarafraz@gmail.com

<sup>1</sup> Therapeutics Research Centre, University of South Australia, Adelaide, Australia  
<sup>2</sup> Faculty of Chemical, Petroleum and Gas Engineering, Semnan University, Semnan, Iran  
<sup>3</sup> Infectious and Tropical Disease Research Center, Hormozgan Health Institute, Hormozgan University of Medical Sciences, Bandar Abbas, IR, Iran  
<sup>4</sup> Student Research Committee, Hormozgan University of Medical Sciences, Bandar Abbas, IR, Iran

UV–visible spectrophotometer. X-ray diffraction analysis further confirmed that the AgNPs were composed of highly crystalline Ag. Transmission electron microscopy analysis revealed that most the AgNPs were in spherical shape with mean diameter about 15 nm. Although they synthesized a relatively pure Ag from by a new method, they did not investigate the thermal performance of the silver Ag.

In another study, Benakashani et al. [11] reported the synthesis of silver nanoparticles by reducing the silver ions present in the solution of silver nitrate by the cell free aqueous extract of *Capparis spinosa* leaves. Silver nanoparticles (AgNPs) were successfully synthesized using *C. spinosa* extract and the nature of synthesized nanoparticles was analyzed by UV–Vis spectroscopy, transmission electron microscopy, X–ray diffraction and Fourier transform infrared spectroscopy. The antimicrobial effect of NPs produced *C. spinosa* was studied using different pathogenic bacteria such as *Escherichia coli*, *Salmonella typhimurium*, *Staphylococcus aureus* and *Bacillus cereus*. Despite the antibacterial activity of Ag particles, they did not report any information on its heat transfer application.

Salari et al. [9] investigated a procedure for the synthesis of the silver nanoparticles. In this research, silver nanoparticles (SNPs) were synthesized through bio-reduction of silver ions using the *Spirogyra varians*. The structure and morphology of SNPs were characterized by UV–visible spectroscopy, X-ray diffraction (XRD) pattern, scanning electron microscopy (SEM) and Fourier Transform Infra-Red (FTIR). These nanoparticles indicated an absorption peak at 430 nm in the UV–visible spectrum. The crystallite average size was estimated about 17.6 nm and SEM image confirmed synthesis of relatively uniform nanoparticles. The antibacterial effect of SNPs was also tested on several micro-organisms by measuring the inhibition zone. However, they did not consider the thermal application of the Ag particles.

A deep look inside the available literature reveals that metallic nanoparticles are capable of being used in thermal systems due to the significant thermal conductivity of the particles [51–56]. For this purpose, solid particles with average size of 0–100 nm are dispersed into the traditional coolant such as water. In order to prevent the deposition of solid particles, stabilizing process are performed which includes different techniques. The prepared mixture is called nanofluid, which has been introduced by Choi [12]. Therefore, silver nanoparticles can potentially be used for thermal application and medical implementations.

In this work, silver nanoparticles are produced using plant extraction method. Particles are produced at different sizes and their antibacterial activity, thermal performance and rheological behaviour is experimentally investigated. The produced particles are characterized using thermal conductivity test (performed with Decagon KD2 Pro), ultraviolet visible spectroscopy (performed with Shimadzu 2600), x ray diffraction (performed with Thermo-Fisher instrument), Scanning

Electron Microscopy (SEM) imaging, Digital light scattering (performed with Horiba instrument) and zeta potential measurement tests (performed with zetasizer Malvern Co.). The zone of inhibition is measured for the antibacterial property analysis of the produced particles using an accurate calliper (purchased from Mitutoyo Co.).

## 2 Materials and methods

### 2.1 Materials

Silver nitrate was used as purchased from Sigma Aldrich Co. Fresh green tea leaves were collected from the northern part of Guilan, Iran. Three times distilled water was purchased from Sareer Teb Chemical Co. and was used for washing, dispersing and dilution of the solutions.

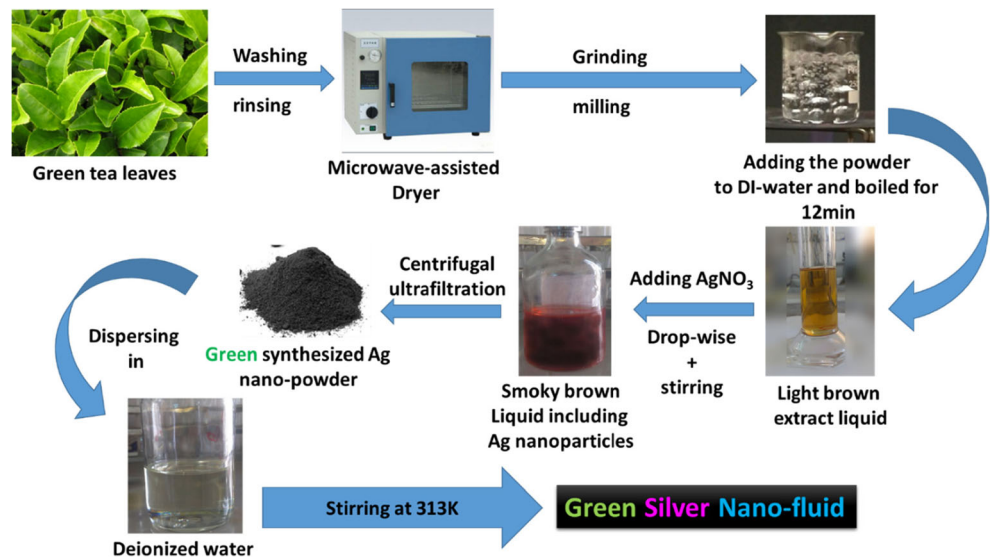
### 2.2 Preparation of the tea extract

As a reducing agent, tea green leaves were used. First the leaves were separated from the sprout and branches, washed, chopped and dried at 298 K. Using a grinder, the dried leaves were powdered. About 14.8 g of green tea leaves powder was added to 100 mL deionized water in a flask. The mixture was boiled for 7–10 min, then was quenched, screened, filtered and kept in 0–4 °C. Then total organic carbon (TOC) content of tea extract was evaluated and analysed using (TOC-Dohrmann, Teledyne), which was approximately 18.97 g/L.

### 2.3 Synthesis of silver nanoparticles

About 750 mL of silver nitrate (10 mM) was added drop wise into the 25 mL of prepared tea extract, while it was gently agitated using magnetic stirrer with the speed of 800 rpm for 120 min at 30–50 °C. Ag nanoparticles were concentrated and purified by centrifugal ultrafiltration and then rinsed and dried. Formation of Ag nanoparticles was indicated by the appearance of signature brown colour of the solution, which is in a good agreement with observations carried out by Yu et al. [13]. Figure 1 shows the synthesis process for producing the silver nanoparticles. It is noteworthy that rate of addition of AgNO<sub>3</sub> droplets into the tea extract is very important. Increasing the rate of addition, especially when accompanied with agitation results in decreased particle size. Therefore, depending on the rate of addition of AgNO<sub>3</sub> droplets, different sample sizes were obtained. The samples were then dried and were sent for characterizing and determining the properties. In this study, three different samples with nominal sizes of 25 nm, 45–50 nm and 75 nm were examined. Nanofluids were prepared at different weight concentrations of 0.1–0.4%. To prepare the nanofluids, following steps were performed:

**Fig. 1** Process implemented for the production of Ag nanoparticles



Initially, desired mass of synthesized nanoparticles was weighed using accurate mass balancer. Then desired mass of base fluid was weighed and then surfactant at the required amount was added into the base fluid. Then, particles were added into the water while it was agitated in a clean flask.

In order to achieve the highest stability of nanofluids, different techniques including the pH control, sonication and adding the surfactant were implemented. Results demonstrated that silver nanoparticles can be stable up to 72 days if right conditions were met during the preparation.

### 3 Results and discussion

#### 3.1 Digital light scattering

Horiba DLS analyser for three different samples at temperature 298 K. Measuring the nanoparticle size were performed three times to ensure about reproducibility and repeatability of the data. Particle size distributions of the samples are demonstrated in Fig. 2. As can be seen, the obtained peaks are not broad but hit the approximate value of 25 nm, 50 nm and 75 nm for samples #1, #2 and #3, respectively. For sample #3, as residence time between the contact phases (droplets of  $\text{AgNO}_3$  and tea extract) is quite sufficient and particles have enough time to grow inside the bulk of the mixture. Therefore, peak of distribution related to the particle size is wider than that of obtained for nanoparticles with 45 nm and 25 nm.

#### 3.2 X ray diffraction test

Figure 3 shows the result of x ray diffraction test for sample #3 at 298 K. Results indicate the single-phase silver nanoparticles with a monoclinic structure. This implies that there is no impurity in the sample other than Ag; however, a small peak due to existence of  $\text{AgO}_2$  is also observed which is negligible. Accordingly, no significant peaks of impurities are found in XRD pattern. XRD Diffraction pattern gives information on symmetry size and shape of the particle and purity of particles from peak positions. The average size of the nanoparticles was also measured using Scherrer's eq. [14, 15], which was approximately equal to 65–70 nm that is in a good agreement with that of obtained by SEM image and those results obtained by DLS analyser.

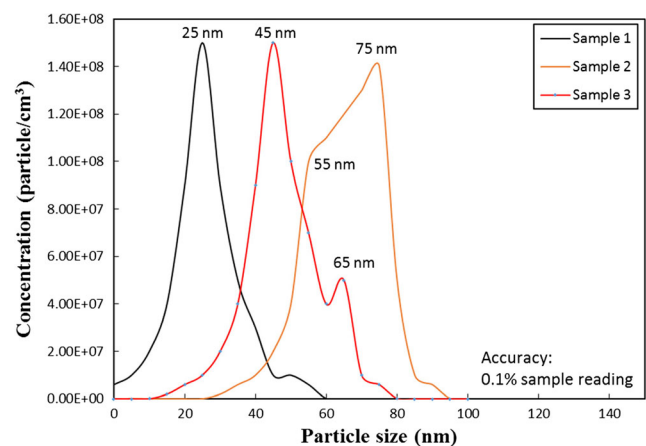


**Fig. 2** Particle size distribution of Ag nanoparticles obtained from DLS particle size

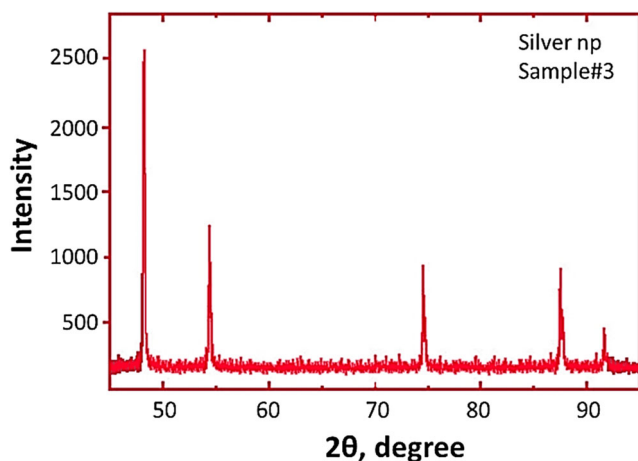


**Fig. 3** X-ray diffraction of silver nanoparticles for sample#3

### 3.3 Scanning electron microscopy

As can be seen in Fig. 4, all prepared nanoparticles are almost identical in terms of morphology and particle size. Neither agglomeration nor clusters were observed in the resulting images. However, in terms of size, particles are different, which implies on this fact that the process introduced for green synthesis of nanoparticles is flexible in producing the nanoparticle with different spectrum of particle size and size distribution profile. Importantly, using stirring and sonication, both crack the agglomeration of particles and makes them uniform [5, 16].

### 3.4 Zeta potential test

Zeta potential is one critical parameter that quantifies the stability of nanofluids. Nanofluids, in principle, are mixture of a liquid such as water and conductive solid particles with nominal size less than 100 nm, which are well-dispersed inside the bulk of the liquid [17, 18]. Due to repulsion and attraction forces between particles, particles-liquid and liquid-liquid molecules, particles tend to deposit inside the container over the extended time. Therefore, after preparing the nanofluid, its stability is examined against time. To enhance the stability of the nanofluids, different techniques can be applied including pH adjustment, sonication and adding surfactant [19]. In this

work, different techniques were used to stabilize the prepared nanofluids. Time-settlement experiments were also conducted to check the stability of the nanofluids. For this experiment, different samples of nanofluids are treated with stabilizing processes and are placed in similar containers for measuring the thickness of sedimentation layer of Ag nanoparticles. It means that sedimentation layer formed at the bottom of the sample vessel is an index for the stability. For a given time, the lower, the thickness of deposited layer, the longer stability is achieved [20–25]. Table 1 shows the summary of the stability experiments.

Zeta potential of the prepared nanofluids were also measured to verify the obtained results by time-settlement experiments. Figure 5 represents the results of zeta potential measured for the three different samples dispersed into deionized water at temperature 298 K. As can be seen, two different regions are defined as unstable and stable regions. The former is the region in which particles tend to form a scale layer at the bottom of the container due to the surface charge of the particle. In fact, in this region, repulsive forces are not high enough to avoid particles from agglomeration inside the liquid. Thus, particles attach to each other and as the result, apparent density increases which leads the particles to be deposited inside the vessel. However, in stable region, particles do not form the agglomerations and clusters and have lower tendency to deposit in comparison with unstable region. Zeta potential is a true criterion for detecting these regions. As can be seen, for weight concentration less than 0.37% and zeta potential less than  $-7.5$  mV, the behaviour of nanofluids falls into stable region, meaning that quantity of sedimentation of nanoparticles is lower than other regions. Noticeably, zeta potential was found to be a function of pH, sonication and surfactant, which are out of goal of this paper to be studied. Overall, the best condition that should be met for the nanofluids to be stable are expressed in Table 1. These conditions are regardless of application of silver nanoparticles and are required to be met.

### 3.5 Ultraviolet-visible spectroscopy (UV-vis)

Due to the surface plasmon resonance of the conduction electrons at the interface between a negative and positive permittivity material induced by the light, the synthesized

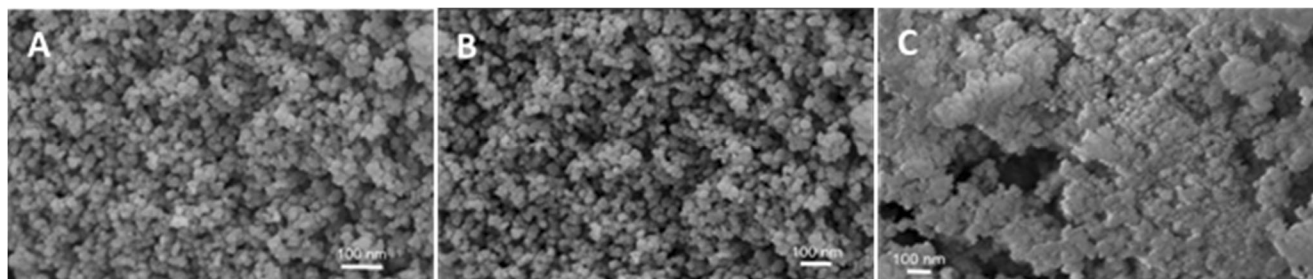


**Fig. 4** Scanning electron microscopic images of Ag nanoparticles at A) 25 nm, B) 45 nm and C) 75 nm sizes

**Table 1** Results of stability experiments and time-settlement tests

Vol.%*	Base fluid	Best sonication time (min)	Sonication Frequency (kHz)	Zeta potential (mV)	Adjusted pH***	Stability Status (max.)
0.001	DI water**	10	36	−85	7.43	stable for 42 days
0.005	DI water	10	36	−63	8.6	stable for 45 days
0.01	DI water	10	40	−45	8.9	stable for 48 days
0.05	DI water	15	40	−39	9.1	stable for 48 days
0.1	DI water	15	40	−28	9.3	stable for 48 days
0.5	DI water	15	40	+12	9.5	unstable
1	DI water	20	40	+16	9.6	unstable

\*For better comparison with the literature, concentrations were reported based on volume fraction on NPs in the base fluid

\*\*deionized water (three times distillate)

\*\*\*buffer solution of 1 mmol HCL and NaOH was used for controlling pH value

nanoparticles were found to be cream and brown colour inside the bulk of the mixture. Fig. 6 shows the results of UV-Vis spectrophotometry obtained from silver nanoparticles (sample#2-50 nm). Results show a peak of absorbance at 455 nm, which is in a good agreement with previous characteristics recorded for silver nanoparticles obtained by green synthesis [26–28]. Also, the spectra shows that a quick bio-reduction is achieved using green tea extract as reducing agent. This finding are in accordance with those reported by [13, 29].

### 3.6 Thermal conductivity measurement

In order to measure the thermal conduction of the produced silver nanoparticles, Decagon KD2 pro device was used. Fig. 7 shows the thermal conduction of the silver nanoparticles measured at room temperature and for different concentration of the silver nanoparticles dispersed in deionized water. For better understanding, an enhancement parameter is

defined as:

$$\text{enhancement ratio} = \frac{k_{nf}}{k_{bf}} \quad (1)$$

In this equation  $k$  is the thermal conductivity measured by KD2 pro device,  $nf$  and  $bf$  stand for nanofluid and base fluid (deionized water here), respectively. In fact, this parameter shows the thermal conductivity of the nanofluid over the base fluid. Presence of solid particles inside the deionized water, due to the Brownian motion, accounts for the enhancement in thermal conductivity of the mixture. Therefore, better thermal performance is expected to be achieved by using the silver/water nanofluid instead of deionized water. To enhance the stability of the nanoparticles and to prevent deposition of particles, different surfactants were used. Fig. 7 shows the variation of thermal conductivity enhancement ratio with the volume fraction of silver nanoparticles and for different surfactants. As can be seen in Fig. 7, the higher enhancement ratio of 1.45 was achieved when Triton-X100 was used as surfactant

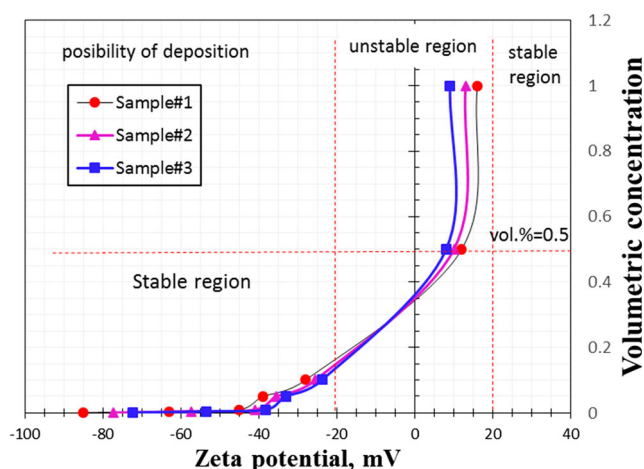


**Fig. 5** Zeta potential of the Ag NPs dispersed in deionized water

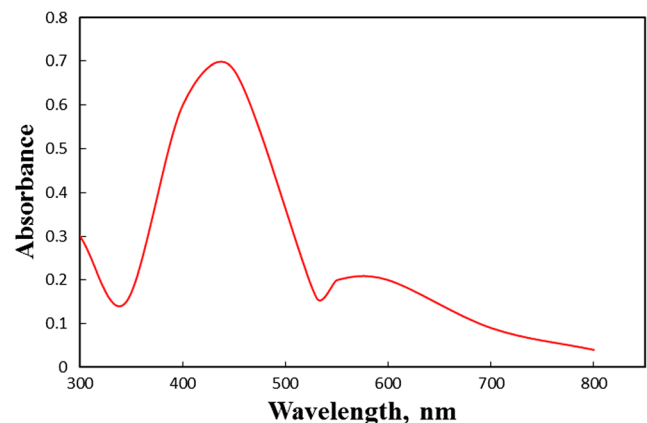
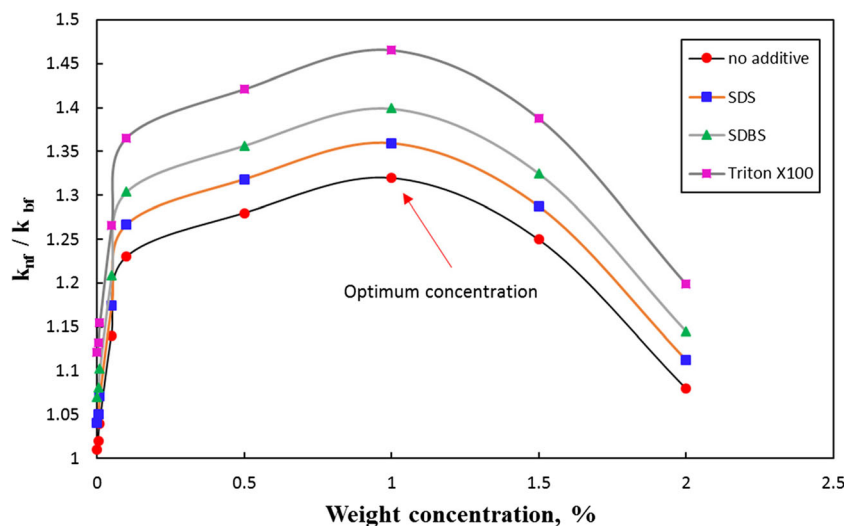


**Fig. 6** Absorption spectra of the nanoparticles. Start wavelength: 300 nm, stop wavelength: 800 nm, pH and other conditions are expressed in Table 1

**Fig. 7** Dependence of thermal conductivity enhancement ratio on concentration of Ag/water nanofluid in presence of different surfactants



and with an increase in the concentration of silver nanoparticles, the enhancement ratio decreased to 1.2. Triton X-100 is followed by Sodium Dodecyl Benzene Sulphonate (SDBS) and Sodium Dodecyl Sulphate (SDS) with maximum enhancement ratio of 1.37 and 1.35, respectively. Noticeably, surfactants were added to the nanofluid at amount of 0.1% of general volume of nanofluid.

Overall, silver nanoparticles enhance the thermal conductivity of the deionized water, when they are dispersed into the water. There is, however, the optimum mass concentration of Ag nanoparticles inside the base fluid was found to be 1%, in which the highest value for thermal conductivity was measured. At higher concentrations, due to the increase in density and instability of the nanofluid, conduction of the liquid decreases. Overall, surfactant is a critical parameter, which influences the stability of Ag/water nanofluid rather than its heat transfer characteristics. These findings imply that silver nanoparticles offer a great potential for thermal and cooling applications, especially in medical services when medical devices need to be cooled down hygienically. As antibacterial features of the silver nanoparticles are explained in the next section.

### 3.7 Analysis of antimicrobial property

Antimicrobial behaviour of the produced nanoparticles against three bacteria species including *Staphylococcus Aureus* (*S. aureus*), *Bacillus*, *Escherichia coli* (*E. coli*), and one yeast, *Bovine Mastitis*, were investigated. For this purpose, these bacteria were grown on agar and silver nanoparticles were supplemented on the very clean agar plates. Nanoparticles with different sizes were used and zone of inhibition was measured accurately using Calipers software and digital ruler for the confirmation of the results and to verify the obtained results. Table 2 shows the antimicrobial effect of silver nanoparticles. Based on these results maximum inhibition zone was registered for nanoparticles with

the smallest size. For instance, for *Bacillus*, inhibition zone is 16 mm when silver NPs with 25 nm nominal size was utilized, while, it is 11 mm when NPs with 75 nm size are used. This is mainly due to the specific surface area of the particles as shown in the literature [13, 31, 32]. As smaller particles have higher specific surface area in comparison with 45 nm and 75 nm, therefore, more areas of particles are exposed to the environment, bacteria and infection zone. Thus, they represented stronger antimicrobial behaviour in comparison with larger nanoparticles. Further studies on anti-cancer properties and activities of these nanoparticles are encouraged [33–41].

### 3.8 Rheological properties

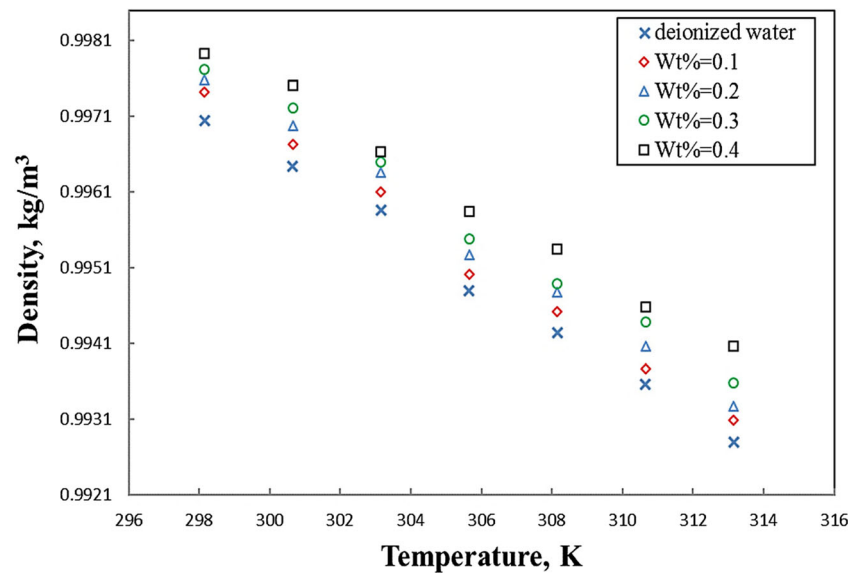
Rheological behaviour of silver nanoparticles determines their application for thermal or medical utilization. Density and viscosity of the silver/water nanofluid influence the Brownian motion and fluid dynamics of the nanofluid. Therefore, these properties were experimentally measured. To measure the variation of density and viscosity with temperature, for each sample, a thermostat water bath was employed. Nanofluid container was placed inside the bath

**Table 2** Antibacterial effect and zone of inhibition for different Ag nanoparticles and for different bacteria

Nanoparticle	Zone of inhibition			
	<i>E. coli</i>	<i>Bacillus</i>	<i>S. aureus</i>	Yeast
25 nm	16 ± 0.1*	14 ± 0.1	14 ± 0.1	9 ± 0.1
45 nm	13 ± 0.5	12 ± 0.5	11 ± 0.5	8 ± 0.5
75 nm	11 ± 0.1	9 ± 0.1	9 ± 0.1	5 ± 0.1

\*Kline-McKlintock method [30] was used to obtain the uncertainty analysis

**Fig. 8** Variation of density of silver/water nanofluid with temperature and for different concentration of 25 nm silver NPs

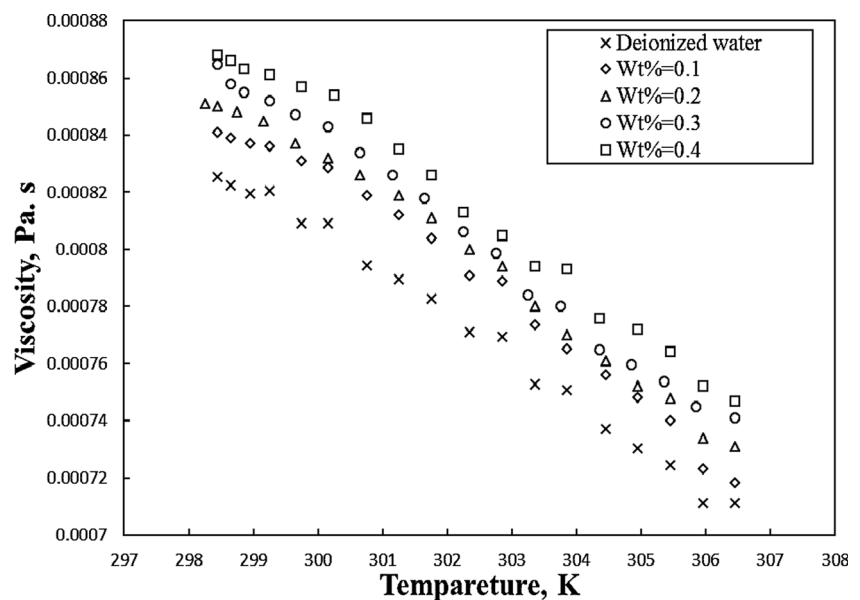


and temperature was set to the target value and let the system reaches to the equilibrium. Then, Brookfield DV+ viscometer and Anton Paar DMA35 densitometer were used to measure the viscosity and density of the nanofluids. By doing this, variation of viscosity and density of nanofluid at each concentration was measured. These steps were repeated for each concentration of nanofluid. Figure 8 shows the variation of density of the silver/water nanofluid with temperature and for different weight concentration of silver nanoparticles in deionized water. The results show that with increasing the temperature, density of the nanofluid slightly decreases. For instance, for wt.% = 0.4, density only decreases 0.4% from 298 K to 313 K. However, increasing the concentration of particles results in the enhancement of the density of

nanofluid. This is mainly due to the presence of the nanoparticles inside the bulk of fluid which increases the mass of the unit volume of nanofluids [42, 43]. Noticeably, increasing the concentration of nanoparticles not only enhances the density of nanofluid but also intensifies the scale formation of the particles. Therefore, depending on the application of the nanofluid, concentration should be optimized [43].

Figure 9 shows the variation of viscosity with temperature of the fluid and concentration of the nanoparticles. As can be seen, presence of particles inside the base fluid leads to the enhancement of the viscosity of the nanofluid. More importantly, temperature decrease the viscosity of the nanofluid, meaning that silver/water nanofluid can present more reasonable thermal performance at high temperature conditions

**Fig. 9** Variation of viscosity of silver/water nanofluid with temperature and for different concentration of 25 nm silver NPs



rather than low temperature. Likewise, when viscosity of the nanofluid increases, it leads the pressure drop inside the pipes, pumps or any convective systems to be increased, which should carefully be considered [44, 45]. This has already been in the literature in boiling and convective systems [46–50].

#### 4 Conclusions

Experimental study on the green synthesis of silver nanoparticle was conducted and following conclusions were drawn:

- Green tea liquor was found to extract the silver from  $\text{AgNO}_3$  and size of the produced particles was found to be a direct function of residence time between phase contacts (drops of  $\text{AgNO}_3$  and green tea liquor). The lower the rate of adding  $\text{AgNO}_3$ , the larger nanoparticles were produced.
- Silver nanoparticle when dispersed in deionized water showed an approximate enhancement of 45% over the base fluid for thermal conductivity, which implied on this fact that silver/water nanofluid offers a great potential for cooling applications.
- Silver nanoparticles showed a great potential for antibacterial activity, however, depending on the size of the particles, antibacterial activity can be intensified or deteriorated. The smaller the particle size, the higher specific surface area and as a result higher anti-microbial behaviour.
- In terms of conductivity, results demonstrated that there is an optimum concentration value for the nanofluid, which was found to be 1% (by weight) for this work.

**Acknowledgements** Authors of this work tend to appreciate Bandar Abbas medical science group, Semnan University and University of Malaya for sharing their facilities. Financial supports of Iran nanotechnology initiative council is acknowledged.

#### Compliance with ethical standards

**Conflict of interest** Authors of this work declare that there is no conflict of interest regarding this paper.

#### References

1. Fedlheim DL, Foss CA (2001) Metal nanoparticles: synthesis, characterization, and applications. CRC press, Boca Raton
2. Cao G (2004) Synthesis, properties and applications. World Scientific, Singapore
3. Poole CP Jr, Owens FJ (2003) Introduction to nanotechnology. John Wiley & Sons
4. Das R, Gang S, Nath SS (2011) Preparation and antibacterial activity of silver nanoparticles. *J Biomater Nanobiotechnol* 2:472
5. Sarafraz M, Hormozi F, Peyghambarzadeh S (2014) Thermal performance and efficiency of a thermosyphon heat pipe working with a biologically ecofriendly nanofluid. *Int Commun Heat Mass Trans* 57:297–303
6. Devaraj P, Kumari P, Aarti C, Renganathan A (2013) Synthesis and characterization of silver nanoparticles using cannonball leaves and their cytotoxic activity against MCF-7 cell line. *J Nanotechnol* 2013
7. Thuc DT, Huy TQ, Hoang LH, Tien BC, Van Chung P, Thuy NT, Le A-T (2016) Green synthesis of colloidal silver nanoparticles through electrochemical method and their antibacterial activity. *Mater Lett*
8. Kalwar K, Sun W-X, Li D-L, Zhang X-J, Shan D (2016) Coaxial electrospinning of polycaprolactone@ chitosan: characterization and silver nanoparticles incorporation for antibacterial activity. *React Funct Polym* 107:87–92
9. Salari Z, Danafar F, Dabaghi S, Ataei SA (2014) Sustainable synthesis of silver nanoparticles using macroalgae *Spirogyra varians* and analysis of their antibacterial activity. *J Saudi Chem Soc* 20:459
10. Wang L, Liu C-C, Wang Y-Y, Xu H, Su H, Cheng X (2016) Antibacterial activities of the novel silver nanoparticles biosynthesized using *Cordyceps militaris* extract. *Curr Appl Phys* 16:969–973
11. Benakashani F, Allafchian A, Jalali S (2016) Biosynthesis of silver nanoparticles using *Capparis spinosa* L. leaf extract and their antibacterial activity. *Karbala Int J mod Sci*
12. Eastman JA, Choi S, Li S, Yu W, Thompson L (2001) Anomalous increased effective thermal conductivities of ethylene glycol-based nanofluids containing copper nanoparticles. *Appl Phys Lett* 78: 718–720
13. Sun Q, Cai X, Li J, Zheng M, Chen Z, Yu C-P (2014) Green synthesis of silver nanoparticles using tea leaf extract and evaluation of their stability and antibacterial activity. *Colloids Surf A Physicochem Eng Asp* 444:226–231
14. Hammond C, Hammond C (2009) The basics of crystallography and diffraction. University Press Oxford, Oxford
15. Warren BE (1969) X-ray diffraction. Courier Corporation, New York
16. Sarafraz M, Hormozi F (2014) Experimental study on the thermal performance and efficiency of a copper made thermosyphon heat pipe charged with alumina–glycol based nanofluids. *Powder Technol* 266:378–387
17. Sarafraz M, Peyghambarzadeh S (2012) Nucleate pool boiling heat transfer to  $\text{Al}_2\text{O}_3$ -water and  $\text{TiO}_2$ -water nanofluids on horizontal smooth tubes with dissimilar homogeneous materials. *Chem Biochem Eng Q* 26:199–206
18. Sarafraz M, Hormozi F (2014) Scale formation and subcooled flow boiling heat transfer of  $\text{CuO}$ -water nanofluid inside the vertical annulus. *Exp Thermal Fluid Sci* 52:205–214
19. Nikkiah V, Sarafraz M, Hormozi F, Peyghambarzadeh S (2015) Particulate fouling of  $\text{CuO}$ -water nanofluid at isothermal diffusive condition inside the conventional heat exchanger-experimental and modeling. *Exp Thermal Fluid Sci* 60:83–95
20. Sarafraz M, Hormozi F, Kamalgharibi M (2014) Sedimentation and convective boiling heat transfer of  $\text{CuO}$ -water/ethylene glycol nanofluids. *Heat Mass Transf* 50:1237–1249
21. Sarafraz M, Hormozi F (2016) Comparatively experimental study on the boiling thermal performance of metal oxide and multi-walled carbon nanotube nanofluids. *Powder Technol* 287:412–430
22. Sarafraz M, Hormozi F, Peyghambarzadeh S (2015) Role of nanofluid fouling on thermal performance of a thermosyphon: are nanofluids reliable working fluid? *Appl Therm Eng* 82:212–224
23. Salari E, Peyghambarzadeh S, Sarafraz M, Hormozi F, Nikkiah V (2017) Thermal behavior of aqueous iron oxide nano-fluid as a coolant on a flat disc heater under the pool boiling condition. *Heat Mass Transf* 53:265–275
24. Sarafraz M, Arya A, Nikkiah V, Hormozi F (2017) Thermal performance and viscosity of biologically produced silver/coconut oil Nanofluids. *Chem Biochem Eng Q* 30:489–500



25. Salari E, Peyghambarzadeh M, Sarafraz MM, Hormozi F (2016) Boiling heat transfer of alumina Nano-fluids: role of nanoparticle deposition on the boiling heat transfer coefficient. *Periodica Polytech Chem Eng* 60:252–258
26. Irvani S (2011) Green synthesis of metal nanoparticles using plants. *Green Chem* 13:2638–2650
27. Bar H, Bhui DK, Sahoo GP, Sarkar P, De SP, Misra A (2009) Green synthesis of silver nanoparticles using latex of *Jatropha curcas*. *Colloids Surf A Physicochem Eng Asp* 339:134–139
28. Vilchis-Nestor AR, Sánchez-Mendieta V, Camacho-López MA, Gómez-Espinosa RM, Camacho-López MA, Arenas-Alatorre JA (2008) Solventless synthesis and optical properties of au and ag nanoparticles using *Camellia sinensis* extract. *Mater Lett* 62: 3103–3105
29. Banerjee P, Satapathy M, Mukhopahayay A, Das P (2014) Leaf extract mediated green synthesis of silver nanoparticles from widely available Indian plants: synthesis, characterization, antimicrobial property and toxicity analysis. *Bioresour Bioprocessing* 1:1
30. Kline SJ, McClintock F (1953) Describing uncertainties in single-sample experiments. *Mech Eng* 75:3–8
31. Sotiriou GA, Teleki A, Camenzind A, Krumeich F, Meyer A, Panke S, Pratsinis SE (2011) Nanosilver on nanostructured silica: antibacterial activity and ag surface area. *Chem Eng J* 170:547–554
32. Park S-J, Jang Y-S (2003) Preparation and characterization of activated carbon fibers supported with silver metal for antibacterial behavior. *J Colloid Interface Sci* 261:238–243
33. Aryanpour N, Mansouri-Torshizi H, Nakhjavan M, Shirazi FH (2012) Cytotoxicity of diimine palladium (II) complexes of alkylthiocarbamate derivatives on human lung, ovary and liver cells. *Iran J Pharm Res* 11:689–695
34. Ashtarinezhad A, Shirazi FH, Vatanpour H, Mohamadzadehasl B, Panahyab A, Nakhjavani M (2014) FTIR-microspectroscopy detection of metronidazole teratogenic effects on mice fetus. *Iran J Pharm Res* 13:101–111
35. Ebrahim K, Vatanpour H, Zare A, Shirazi FH, Nakhjavani M (2016) Anticancer activity of Caspian cobra (*Naja Naja oxiana*) snake venom in human cancer cell lines via induction of apoptosis. *Iran J Pharm Res* 15:101–112
36. Jamali B, Nakhjavani M, Hosseinzadeh L, Amidi S, Nikounezhad N, Shirazi FH (2015) Intracellular GSH alterations and its relationship to level of resistance following exposure to cisplatin in cancer cells. *Iran J Pharm Res: IJPR* 14:513
37. Nakhjavani M, Nikounezhad N, Ashtarinezhad A, Shirazi FH (2016) Human lung carcinoma reaction against metabolic serum deficiency stress (autumn 2016). *Iran J Pharm Res* 15:817
38. Nakhjavani M, Vatanpour H, Shahriari F, Mohamadzadehasl B (2016) Lifesaving effect of lidocaine on *Odontobuthos Doriae* scorpion envenomation in mice. *American J Pharm-Tech Research* 6: 179
39. Nakhjavani M, Zarghi A, Shirazi FH (2014) Cytotoxicity of selected novel chalcone derivatives on human breast, lung and hepatic carcinoma cell lines. *Iran J Pharm Res* 13:953–958
40. Nikounezhad N, Nakhjavani M, Shirazi FH (2016) Generation of cisplatin-resistant ovarian cancer cell lines. *Iran J Pharm Sci* 12:11–20
41. Shirazi FH, Zarghi A, Ashtarinezhad A, Kobarfard F, Nakhjavani M, Anjidani N, Zendehtdel R, Arfaiee S, Shoeibi S, Mohebi S (2011) Remarks in successful cellular investigations for fighting breast cancer using novel synthetic compounds. INTECH Open Access Publisher, Croatia
42. Godson L, Raja B, Lal DM, Wongwises S (2010) Experimental investigation on the thermal conductivity and viscosity of silver-deionized water nanofluid. *Exp Heat Transfer* 23:317–332
43. Wang X, Xu X, Choi SU (1999) Thermal conductivity of nanoparticle-fluid mixture. *J Thermophys Heat Transf* 13:474–480
44. Vajjha RS, Das DK (2012) A review and analysis on influence of temperature and concentration of nanofluids on thermophysical properties, heat transfer and pumping power. *Int J Heat Mass Transf* 55:4063–4078
45. Gherasim I, Roy G, Nguyen CT, Vo-Ngoc D (2011) Heat transfer enhancement and pumping power in confined radial flows using nanoparticle suspensions (nanofluids). *Int J Therm Sci* 50:369–377
46. Sarafraz MM, Peyghambarzadeh SM, Alavi Fazel SA, Vaali N (2013) Nucleate pool boiling heat transfer of binary nano mixtures under atmospheric pressure around a smooth horizontal cylinder. *Period Polytech Chem Eng* 57(1–2):71
47. Sarafraz MM, Hormozi F, Peyghambarzadeh SM (2016) Pool boiling heat transfer to aqueous alumina nano-fluids on the plain and concentric circular micro-structured (CCM) surfaces. *Exp Thermal Fluid Sci* 72:125–139
48. Sarafraz MM, Hormozi F, Peyghambarzadeh SM (2015) Role of nanofluid fouling on thermal performance of a thermosyphon: Are nanofluids reliable working fluid? *Appl Thermal Eng* 82:212–224
49. Sarafraz MM, Hormozi F, Peyghambarzadeh SM, (2014) Thermal performance and efficiency of a thermosyphon heat pipe working with a biologically ecofriendly nanofluid. *Int Commun Heat Mass* 57:297–303
50. Sarafraz MM, Peyghambarzadeh SM, Vaali N (2012) Subcooled flow boiling heat transfer of ethanol aqueous solutions in vertical annulus space. *Chem. Ind. Chem. Eng. Q* 18(2):315–327
51. Sarafraz MM, Kiani T, Hormozi F (2016) Critical heat flux and pool boiling heat transfer analysis of synthesized zirconia aqueous nanofluids. *Int Commun Heat Mass* 70:75–83
52. Sarafraz MM (2012) Nucleate pool boiling of aqueous solution of citric acid on a smoothed horizontal cylinder. *Heat Mass Transf.* 48(4):611–619
53. Sarafraz MM, Hormozi F, Nikkhah V (2016) Thermal performance of a counter-current double pipe heat exchanger working with COOH-CNT/water nanofluids. *Exp Thermal Fluid Sci* 78:41–49
54. Sarafraz MM, Peyghambarzadeh SM, Alavi Fazel SA, Vaali N (2013) Nucleate pool boiling heat transfer of binary nano mixtures under atmospheric pressure around a smooth horizontal cylinder. *Period Polytech Chem Eng* 57(1–2):71
55. Sarafraz MM, Hormozi F (2016) Comparatively experimental study on the boiling thermal performance of metal oxide and multi-walled carbon nanotube nanofluids. *Powder Technol* 287: 412–430
56. Sarafraz MM, Hormozi F (2016) Experimental investigation on the pool boiling heat transfer to aqueous multi-walled carbon nanotube nanofluids on the micro-finned surfaces. *Int J Therm Sci* 100:255–266